Journal of Fluorescence, Vol. 11, No. 4, December 2001 (© 2002)

Fluorescence Spectroscopic Studies on Phase Heterogeneity in Lipid Bilayer Membranes

Winchil L. C. Vaz[1,3] and Eurico Melo[2]

There is a growing interest in functional membrane heterogeneity on the mesoscopic (several tens to hundreds of molecular dimensions) scale. However, the physical–chemical basis for this sort of heterogeneity in membranes is not entirely clear. Unambiguous methods to demonstrate that the cell plasma membrane and other cellular membranes are in fact heterogeneous on the mesoscopic level are also not generally available. Fluorescence techniques do, however, provide excellent tools for this purpose. In particular, the emerging techniques of scanning near-field optical microscopy and single-molecule fluorescence microscopy hold a great deal of promise for the near-future. All these methods require the use of fluorescent probes (lipids and/or proteins) and a clear definition of how these probes partition between domains of coexisting membrane phases. The development of the concept of membrane heterogeneity over the years since the first proposal of the "fluid mosaic" model is reviewed briefly. The use of lipid-binding proteins in experimental protocols for the labeling of membranes with fluorescent lipid amphiphiles as monomers in aqueous solutions at concentrations well above their critical aggregation concentrations is discussed. The methods of fluorescence spectroscopy available to the cell biologist for determining probe partition coefficients for partitioning between coexisting membrane phases are reviewed in some detail, as is the relevant theoretical and experimental work reported in the literature.

KEY WORDS: Fluorescence probes; membrane heterogeneity; partition coefficients; lipid-binding proteins.

INTRODUCTION

Our present understanding of the way biological membranes function owes a considerable debt to the vast amount of literature generated by the scientific community after the proposal of the "fluid mosaic" model [58] for biomembrane structure and dynamics. A very considerable fraction of this literature was devoted to the properties of lipid bilayer membranes since these were understood, within the context of the fluid mosaic model, to be the base structures of the biological membrane. It was natural that the process should also have led, as it did, to a considerable increase in our understanding of the properties of various hydrated phospholipid mesophases. Today, almost 30 years since the proposal of the fluid mosaic model, the attention of the interested scientific community is being dominated by the relevance of the physical structure of the phospholipid bilayer matrix of the biological membrane to cell physiology.

From a physical–chemical perspective we may view the biological membrane as a quasi-two-dimensional fluid solution that forms an interface between two bulk three-dimensional aqueous solutions: the intracellular solution, or cytoplasm, and the extracellular solution; or two intracellular compartments. The quasi-two-dimensional fluid solution that we call the membrane can be viewed as a fluid solvent composed of two leaflets, each with the

[1] Departamento de Química, Universidade de Coimbra, 3004-535 Coimbra, Portugal.
[2] Instituto de Tecnologia Química e Biológica, Universidade Nova de Lisboa, 2784-505 Oeiras, and Instituto Superior Técnico, 1049-001 Lisboa, Portugal.
[3] To whom correspondence should be addressed. Fax: Int + 351 239827703. E-mail: wvaz@ci.uc.pt

1053-0509/01/1200-0255/0

thickness of the mean length of the constituting lipids, in which all other membrane components are dissolved or to which they are adsorbed due to the effect of a variety of forces which range from purely surface electrostatics to solvation of limited parts of the solute molecules (lipid-attached proteins or amphipathic helices, for example). Viewed in this manner, it becomes important to understand the nature and properties of the solvent. One of the first questions that naturally arises is whether or not the solvent is homogeneous. The fact that each leaflet of the lipid bilayer of a membrane is composed of several chemical constituents [45] leads us immediately to consider that the solvent could be a physically heterogeneous system [19]. Although this was not explicit in the proposal of the fluid mosaic model, the possibility that "some significant fraction of the phospholipid is physically in a different state from the rest of the lipid" was not specifically excluded from the proposal. Very early work from the laboratories of McConnell [77] and Sturtevant [36] clearly established that lipid miscibility in hydrated phospholipid bilayers was often nonideal and that this nonideality sometimes extended to states in which all constituents were in a fluid state. Since that pioneering work, the publication of several phase diagrams of hydrated lipid bilayers composed of binary or higher-order mixtures of lipids [37] has justified the conclusion that "lipid miscibility in a lipid bilayer is more the exception than the rule" [67].

A heterogeneous lipid bilayer as the basic matrix of a biological membrane is an attractive concept in that it could lead to an effective "compartmentalization" of the membrane, a phenomenon that has its counterpart in the whole cell, with well-documented consequences for cellular metabolism and physiology. It is, therefore, not surprising that proposals for a membrane structure with coexisting immiscible domains at the level of the lipid bilayer arise at a very early stage in the post–fluid mosaic era [24,26,27,44,62]. Interpretation of our results on the long-range diffusivity of fluorescent lipid derivatives in multiphase lipid bilayers in terms of two-dimensional percolation [1–3,11,65–67,70,71] led us to propose that biomembranes could make use of the interesting consequences of phase heterogeneity and the resultant component compartmentalization [68] if they were themselves "domain mosaics" [40,63,66–69], and a modification of the fluid mosaic model was proposed to include these concepts [66,69] (see Fig. 1).

Differential solubilization of plasma membranes in detergent solutions has been used increasingly as evidence in support of the existence of cell membrane heterogeneity. This differential solubilization results in the isolation of sphingolipid- and cholesterol-rich bilayer structures, insoluble at low temperatures in Triton X-100 micelles, which have been equated with sphingolipid- and cholesterol-rich domains, termed "rafts," in the original membranes (for reviews on rafts see Refs. 8–10,25,50,56, and 57). While the conclusion that detergent insolubility necessarily means plasma membrane heterogeneity resulting from lipid immiscibility may be questioned on the basis of very fundamental principles of phase behavior, the recent literature in cell biology and biophysics seems to have accepted rafts as a fact, and almost every result that can be attributed to a heterogeneity of a biological membrane [48,52] is today attributed to rafts in one form or another. Be that as it may, it is gratifying to see that there is a generalized acceptance of functional heterogeneity in cell membranes, something that, retrospectively, probably should never have been doubted and, as mentioned above, has been suggested by several workers since the early 1970s.

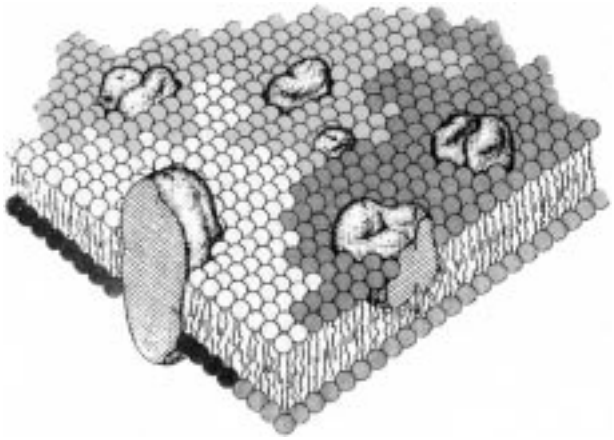

Fig. 1. A modified version of the fluid mosaic model of Singer and Nicolson (1972), which includes the concept that phase separations in the cellular membranes could result in a heterogeneous system with coexistence of domains of several different kinds of lipid phases. Adapted with permission from Vaz and Almeida (1993) and Vaz (1994).

Having accepted that biological membranes may be heterogeneous, it becomes incumbent to demonstrate this in an unambiguous and direct manner. This is particularly important if functional consequences are attributed to membrane heterogeneity. Direct demonstration of a structure usually involves visualization of the same by some sort of microscopy. For biological membrane structures with dimensions that are smaller than the limits of optical resolution, electron microscopy [generally after freeze-fracture (see, e.g., Ref. 62)], atomic force microscopy [20], and near-field scanning optical microscopy [21,23] become the methods of choice because of their high resolution. Microscopic techniques that involve measurement of single-particle or domain diffusivities [48,52], while

being relatively straightforward in their interpretation, though not simple to perform, cannot be said to be direct and unambiguous demonstrations of membrane heterogeneity. Besides, in these techniques, it is fundamental to know how the probes used behave within the membrane in which they are being visualized. Electron microscopy and atomic force microscopy provide relatively static views of the system under investigation and require clearly definable differences in surface topology or order (or rigidity, in the case of atomic force microscopy) between the coexistent membrane phases so as to permit them to be distinguished from each other. In the long term, and considering that single living cells are the eventual object of study, near-field scanning optical microscopy seems to provide the best choice for the study of membrane heterogeneity *in situ*. The method is, however, still not at a stage of technical development that makes it generally useful, but this may be only a matter of time. While freeze-fracture electron microscopy and atomic force microscopy do not require probes, near-field scanning optical microscopy does. Its successful utilization is, therefore, also dependent upon the detailed and quantitative characterization of the probe interaction with the membrane phases, and it is this aspect that we review here.

PROBES FOR MEMBRANE MICROSCOPY

Ideally, probes of any sort should be intrinsic to the system under study so that there can be no doubts about perturbative effects. This is, however, usually an utopic requirement, and most useful work has, in the past, been the result of using extrinsic probes whose perturbation of the system is minimal and/or adequately understood. For optical microscopic applications, membrane probes are fluorescent molecules that are attached to the membrane proteins either directly by covalent attachment or indirectly as fluorescently labeled antibodies that specifically bind certain molecules in the membrane. Alternatively the fluorescent molecules partition preferentially into the membrane as a consequence of their apolarity and report on its properties. Fluorescent lipid amphiphiles (FLAs) (see list of abbreviations in the Appendix) fall into this class of membrane "stains." These consist of a fluorophore covalently attached to an amphiphilic carrier which may be (ideally is) a derivative of a membrane lipid. The fluorophore itself may be part of the apolar (acyl chains substituted by an apolar fluorophore such as DPH, pyrene, anthroyl, carbazole, or indole groups) or polar (headgroups are modified using any one of several rather polar fluorophores) portion of the molecule.

The spectral characteristics of the fluorophore should be such as to be clearly distinguishable from cellular autofluorescence, which generally implies molecules that absorb and fluoresce at wavelengths above 500 nm. A high molar extinction coefficient, emission quantum yield, and photochemical stability are also desirable characteristics. Ideal excited-state lifetimes and the limiting polarization, r_0, of the fluorophore depend very much upon which characteristic of the membrane microenvironment is to be probed. The charge of the fluorescent derivative in the polar membrane interface is also a characteristic that may not be ignored when membrane compositions that include charged lipids or domains rich in charged lipid constituents are being examined. For cellular membranes this becomes a very important property of the fluorescent "stain."

If staining is done with FLAs, i.e., amphiphiles, whether or not derived from membrane lipids, the nature of the apolar portion of the molecule is of importance since this may determine the partitioning of the probe between ordered and disordered membrane domains and thus determine their utility as stains for detecting and quantitatively describing this type of phase coexistence (see below).

HOW ARE AMPHIPHILES ADDED TO CELLULAR MEMBRANES?

Fluorescent lipid amphiphiles (FLAs) are the ideal stains for cell membranes when the visualization of coexisting lipid phases in them is desired [5,29]. As a simplistic first approximation, an aqueous solution of the FLA may be added to a cell culture, the expectation being its spontaneous association with the cell membrane. The amount of FLA that associates with the cell membranes will be a function of its total concentration in the aqueous phase and the membrane/water partition coefficient (K_P), which will be different for different amphiphiles. But amphiphiles form molecular aggregates (micelles, microcrystals) at some critical aggregation concentration (CMC or solubility product, if sparingly soluble) which depends upon the nature of the polar and apolar portions of the molecule and can be quite low. In fact, the more similar an amphiphile is to a naturally occurring lipid in its behavior, the lower its CMC is likely to be. Intense local staining will result if an aggregate comes in contact with a cell surface and fuses with it [4]. Obstruction of free lateral diffusion of the FLA in the plane of the surface, which we may suppose to be the plasma membrane, will then result in an apparent membrane inhomogeneity that is not a physical property of the membrane but an artifact

of the staining procedure. This problem does not exist, however, if the stain is able to access the target membrane only as a monomer. In practice this will be the case if the FLA is added to the target membrane as an aqueous solution at a concentration below its CMC. Such a procedure has two drawbacks: (1) the CMC could be too low to permit significant staining within a practically useful time; and (2) the higher the value of the CMC, the lower the value of K_P is likely to be, which means that the likelihood of the FLA desorbing from the membrane surface and eventually reinserting into some other membrane or membrane phase could be quite high. Also, the nonnegligible concentration of FLA in the aqueous phase may give rise to a nondesirable fluorescence background. This would imply that the stain will eventually (the process can be quite rapid, depending on the desorption and association rate constants) be distributed in all accessible membranes and not be limited to just the targeted one.

Another approach to the monomerization of an FLA in aqueous solution is to present it as a protein-bound species.[4] In this case the two FLA species encountered in solution are, ideally, the monomer in aqueous solution and the protein-bound form, which are in equilibrium with each other. In general, the total amount of FLA added to the cells to be stained will typically be based upon the desired level of staining (moles of amphiphile per unit of cell membrane surface), the total membrane area to be stained, and K_P for the amphiphile partitioning between the membrane and the aqueous phases. The amphiphile-binding protein must be at a concentration that, in consideration of the FLA/protein equilibrium association constant, K_A, assures that the concentration of free amphiphile at equilibrium is below its CMC. Using the Mass Action Law for the equilibrium (assuming a single binding site on the protein),

$$A_w + P \overset{K_A}{\rightleftharpoons} PA$$

where A_W, P, and PA are the FLA in aqueous solution, the lipid-binding protein, and the protein–FLA complex; the equilibrium association constant $K_A = [PA]/[A_W][P]$, where the equilibrium concentration of free FLA in aqueous solution $[A_W] = C_A - [PA]$, and the equilibrium concentration of free protein in solution $[P] = C_P - [PA]$; and C_A and C_P are the total concentrations of FLA and protein, respectively. Figure 2 shows the variation of $[A_W]$ as a function of C_A for various values of C_P and K_A. Knowledge of the CMC for the FLA will then permit us to estimate whether or not the goal of its monomerization in aqueous solution has been achieved.

Having monomerized the FLA in aqueous solution, its transfer to the cell surface membrane will depend upon the following competing equilibria:

$$A_w + P \overset{K_A}{\rightleftharpoons} PA$$

$$A_w \overset{K_P}{\rightleftharpoons} A_L$$

The velocities for binding and desorption from the membrane surface can be written

$$v_+ = k_+[A_w]S_L \quad \text{and} \quad v_- = k_-[A_L]S_L \tag{1}$$

and the equilibrium partition coefficient, K_P, for FLA partitioning between the membrane phase and the aqueous phase is given by

$$K_P = \frac{k_+}{k_-} = \frac{[A_L]}{[A_w]} \tag{2}$$

The suffixes + and − refer, respectively, to the binding and desorption processes, k are the rate constants, S_L is the area of the lipid (membrane) phase referred to the total volume of the reaction mixture, and C_S is the surface concentration (moles per unit area) of the FLA in the membrane phase. It can be shown that at equilibrium C_S is related to C_A, C_P, K_A, and K_P by the expression

$$C_A = C_S\left(S_L + \frac{1}{K_P} + \frac{K_A C_P}{K_P + K_A C_S}\right) \tag{3}$$

Figure 3 shows some results for the expected FLA density in the target membrane as a function of the total FLA concentration. The values of the FLA density in the target membrane are relatively insensitive to C_P and K_A.

Determinations of the CMC of amphiphiles in aqueous solutions have been described for values of CMC as low as 10^{-16} [49,60], and the same methodology would, in principle, be applicable to solutions of FLAs as well. A simpler method, however, could be via utilization of the spectroscopic properties of the FLAs themselves since the fluorescence properties are usually different for the monomer in aqueous solution and in the micelle (aggregate). As an example we present the determination of the CMC (4.2×10^{-9} M) of NBD–di$C_{14:0}$PE obtained by simple measurement of the concentration-normalized fluorescence emission intensity as a function of the FLA concentration (Fig. 4) (M. Abreu, unpublished results).

FLAs may also be introduced via metabolic pathways into cell membranes (Ref. 64 and references therein), a method that may merit closer study.

[4] This method is quite generally used and is, to the best of our knowledge, based upon a protocol from the laboratory of Dr. Richard E. Pagano. We are not aware of any quantitative studies concerning the binding of most of the FLA used to albumin or of any quantitative studies concerning the transfer of these albumin-bound amphiphiles from the albumin-binding site to the membrane surface.

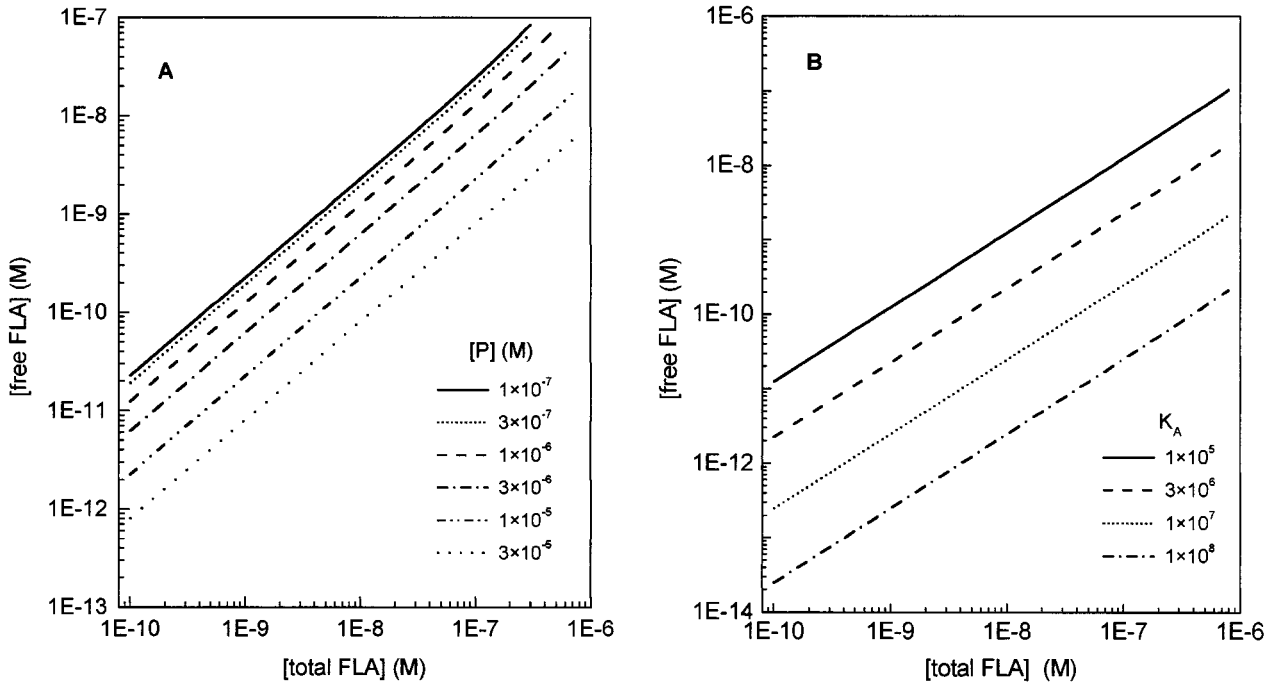

Fig. 2. Effect of an FLA-binding protein upon the equilibrium concentration of the free FLA in aqueous solution (A). The curves are, from bottom to top, for [P] = 3×10^{-5}, 1×10^{-5}, 3×10^{-6}, 1×10^{-6}, 3×10^{-7}, and 1×10^{-7} *M* FLA-binding protein. K_A is assumed to be 1×10^6 in all cases. (B) As a function of the equilibrium association constant for the association of the FLA to the FLA-binding protein. The curves are, from bottom to top, for $K_A = 1 \times 10^8$, 1×10^7, 3×10^6, and 1×10^5. The concentration of the FLA-binding protein is 1×10^{-5} *M* in all cases.

DETERMINATION OF PROBE (STAIN) PARTITIONING BETWEEN COEXISTING MEMBRANE PHASES

Once the FLA stain is in a membrane its distribution within this structure will depend upon its partition coefficient between different coexisting phases. If the membrane has two phases in coexistence and the FLA is totally insoluble in one of them, clearly the FLA will reside exclusively in the second phase and its utility is unambiguous. To the best of our knowledge this extreme situation is obtained only when one of the phases is a pure gel phase (see, e.g., Refs. 28 and 41). For all other situations, when two fluid phases coexist, the FLAs have some finite nonzero value for the interphase partition coefficient, $K_{P(L)}$.

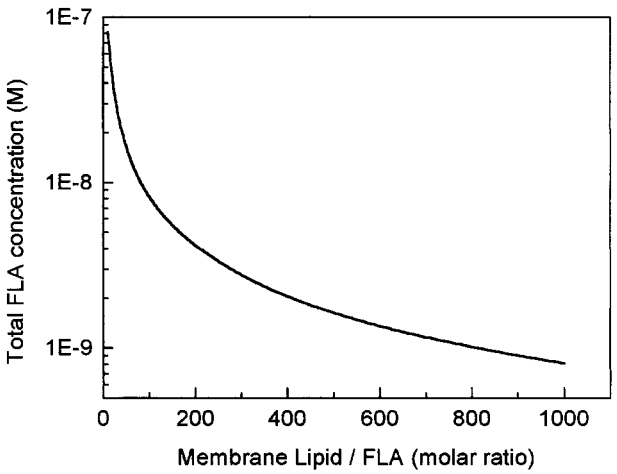

Fig. 3. FLA density in a target membrane as a function of the total FLA concentration. A cell density of 1×10^6 cells/ml, $K_A = 1 \times 10^6$, $K_P = 1 \times 10^8$, and [P] = 1×10^{-5}, *M* were assumed.

It can be imagined that more than two phases could coexist in a given cell plasma membrane. However, the only situation susceptible to an analytical solution concerning which domains have which probe and in what amount is one in which the membrane heterogeneity is assumed to result from just two phases in coexistence with each other. Numerical solutions may, however, be possible for cases in which more than two types of domains coexist. For quantitative examination of natural membrane heterogeneity using FLAs, we have to know the value of $K_{P(L)}$. This can be determined only in a model system that is known to consist of the two phases expected to exist in the target cell membrane. The phase diagram of the model membrane system must also be known.

Davenport [13] has recently reviewed some of the fluorescence spectroscopy techniques that can be used to study the partitioning of fluorophores between coexistent

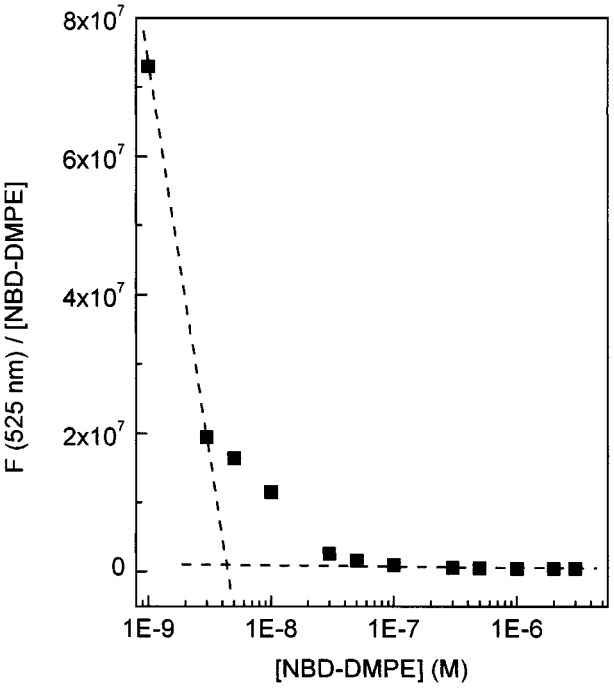

Fig. 4. Determination of the critical aggregation concentration of NBD–di$C_{14:0}$PE. The concentration-normalized fluorescence intensity is defined as the fluorescence intensity measured for a given concentration divided by that concentration. The absorbances of the solutions used for fluorescence intensity measurements are such that the inner filter effect is negligible. Reproduced with the kind permission of Magda Abreu.

phases in membranes. In general, if there are A_i molecules of an FLA in phase i with area fraction x_i, the partition constant, $K_{P(L)}$, is defined as

$$A_2 \overset{K_{P(L)}}{\rightleftharpoons} A_1$$

and is given by

$$K_{P(L)} = \frac{[A_1]}{[A_2]} \tag{4}$$

where $[A_i]$ refer to the concentration of the FLA in a given phase as moles per unit area of that phase, taking the thermodynamic standard state as the unit molar concentration per unit area. Several observable fluorescence parameters can be used to determine $K_{P(L)}$: fluorescence intensity variations at a given wavelength due to spectral shifts and/or quantum yield variations, fluorescence lifetime variations between coexisting phases, decomposition of fluorescence emission spectra arising from FLAs in different phases, differences in the emission anisotropies between different phases, and fluorescence quenching. Quantitative analysis of the experimental results obtained from fluorescence quenching experiments must consider that both the FLA and the quencher have their own specific $K_{P(L)}$ and translational diffusion coefficients. In addition, the unquenched lifetimes of the FLA in the different phases could be different; dimensional effects (in particular, effects related to two-dimensional diffusion and topology of the diffusional space) are likely to make an exact analysis extremely complex. Dynamic quenching of fluorescence also restricts us to the use of FLAs with chromophores that have a long excited-state lifetime if we want to avoid the use of very high quencher concentrations. $K_{P(L)}$ can, in principle, be determined quantitatively by quenching experiments only when quenching in one of the phases is complete and an exclusively static process.

Fluorescence Lifetime. In the absence of other complicating effects the decay of fluorescence, $F(t)$, of an FLA that partitions between two phases follows a double-exponential law:

$$F(t) = a_1 \exp(-t/\tau_1) + a_2 \exp(-t/\tau_2) \tag{5}$$

In the more common case, where multiexponential decay in pure phases is observed, the equations presented hereafter need to be adequately adapted. For reliable amplitudes, a_i, and lifetimes, τ_i, to be extracted, the fluorescence lifetimes in the two phases, determined independently, should be sufficiently distinctive, e.g., $\tau_2/\tau_1 > 1.5$ [34].

Both the absorption and the emission spectra of A may be different in shape and intensity when A is in phases 1 and 2, as in the idealized case represented in Fig. 5, in which the fluorescence intensities measured at λ_{em} have to be corrected for the different absorptions at the excitation wavelength, λ_{ex}, and the emission intensity.

Supposing that the amount of FLA not attached to the membrane is negligible (the emission observed arises only from membrane-bound FLA), and for very low absorbance values, the number of quanta absorbed by the solution, $I_i^{\lambda_{ex}}$, is proportional to the molar absorptivity at the wavelength, $\varepsilon_i^{\lambda_{ex}}$,

$$\begin{aligned} I_1^{\lambda_{ex}} &= \beta \varepsilon_1^{\lambda_{ex}} [A_1] x_1 \\ I_2^{\lambda_{abs}} &= \beta \varepsilon_2^{\lambda_{ex}} [A_2](1 - x_1) \end{aligned} \tag{6}$$

β being a constant of proportionality. The relative intensity of fluorescence emission observed at λ_{em} for $t = 0$ will then be

$$\frac{a_1}{a_2} = \gamma \frac{k_{f1}\, \varepsilon_1^{\lambda_{ex}} [A_1]_1\, x_1}{k_{f2}\, \varepsilon_2^{\lambda_{ex}} [A_2]_2 (1 - x_1)} = \gamma \frac{k_{f1} \varepsilon_1^{\lambda_{ex}}\, x_1}{k_{f2} \varepsilon_2^{\lambda_{ex}} (1 - x_1)} K_{P(L)} \tag{7}$$

where k_{fi} is the radiative rate constant in each environment, obtained from the FLA lifetime and quantum yield

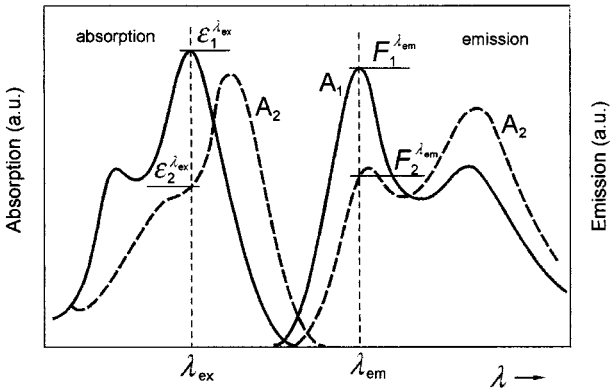

Fig. 5. Idealized absorption and emission spectra of a FLA showing the molar absorptivities, ε_i, at the excitation wavelength, λ_{ex}, and the relative fluorescence intensity, F_i, at λ_{em}.

in the pure phases (by definition, $k_f = \Phi_f/\tau$); $\gamma = y_1^{\lambda_{em}}/y_2^{\lambda_{em}}$ corrects for the intensity of fluorescence at the emission wavelength of component *i*; and $y_i^{\lambda_{em}}$ = fluorescence intensity collected at λ_{em}/total fluorescence intensity of A in phase *i*.

In the region where the two phases coexist the decays of the FLA excited state in each of the coexisting phases follow Eq. (5), and if all the other parameters are known, a global analysis of the biexponential decays imposing the relation between preexponentials from Eq. (7) will have $K_{P(L)}$ as the only adjustable parameter. The proviso that "all the other parameters are known" is, for the present case, difficult to satisfy except when we have experimental evidence that the absorption and fluorescence emission spectra of the FLA do not shift or change in shape with the transfer of the FLA between phases, for which case Eq. (7) is reduced to

$$\frac{a_1}{a_2} = \frac{k_{f1}x_1}{k_{f2}(1 - x_1)} K_{P(L)} \tag{8}$$

The absence of spectral change is a condition that is difficult to observe because, in general, a significant difference in the lifetime results either from a change in the nature of the lowest excited singlet state or from the tuning of the energy of the excited singlet state relative to that of a neighboring triplet state, both implying a large spectral change and, most probably, quite different k_f values.

The method of fluorescence lifetime variation described should be, in the case where Eq. (8) applies, the most expedient of all. In practice, only a restricted number of chromophores allows a reliable and consistent analysis of the decay data obtained, even when the decay from each phase is a clean single exponential and the difference between the two lifetimes is sufficiently large for them to be resolved.

Emission Anisotropy. In analogy with what is done in the fluorescence lifetime method we also observe the fluorescence anisotropy at a given wavelength λ_{em} with excitation at a wavelength λ_{ex}, as represented in Fig. 5. Due to the additivity property of the fluorescence anisotropy [74], the total fluorescence anisotropy, *r*, is

$$r = r_1 f_1 + r_2 f_2 \tag{9}$$

where r_i are the anisotropies of the fluorescence emitted by A_i, and f_i the fraction of the total emission intensity at λ_{em} originating from the molecules in each medium.

In Eq. (9) the fraction of fluorescence emitted by A_i is given by

$$f_i = \frac{F_i^{\lambda_{em}}}{F_1^{\lambda_{em}} + F_2^{\lambda_{em}}}$$

$$= \frac{\varepsilon_i^{\lambda_{ex}}[A_i]x_i\,\Phi_i y_i^{\lambda_{em}}}{\varepsilon_1^{\lambda_{ex}}[A_1]x_1\Phi_1 y_1^{\lambda_{em}} + \varepsilon_2^{\lambda_{ex}}[A_2](1 - x_1)\Phi_2 y_2^{\lambda_{em}}} \tag{10}$$

and in terms of $K_{P(L)}$ it may be rewritten for phase 1 as

$$f_1 = \xi K_{P(L)} \frac{x_1}{1 - x_1} \Big/ \left(1 + \xi K_{P(L)} \frac{x_1}{1 - x_1}\right) \tag{11}$$

where $\xi = \varepsilon_1^{\lambda_{ex}} y_1^{\lambda_{em}} \Phi_1/\varepsilon_2^{\lambda_{ex}} y_2^{\lambda_{em}} \Phi_2$.
The same algebra for phase 2 leads to

$$f_2 = 1/\left(1 + \xi K_{P(L)} \frac{x_1}{1 - x_1}\right) \tag{12}$$

and substituting in (9), we obtain

$$r = \left(r_1 \xi K_{P(L)} \frac{x_1}{1 - x_1} + r_2\right) \Big/ \left(1 + \xi K_{P(L)} \frac{x_1}{1 - x_1}\right) \tag{13}$$

From Eq. (13) the values of r_i are readily obtained if we know ξ, the ratio of the fluorescence intensities at λ_{em} of two samples of pure phases 1 and 2 with the same FLA concentration excited at λ_{ex}. If the isosbestic and isoemissive wavelengths are known, then the best solution is to use them, making $\xi = 1$.

Fluorescence Quantum Yield. Some FLAs have a strong environment-dependent fluorescence quantum yield that is frequently accompanied by a change in the shape of the absorption and emission spectra. From Eq. (6) we may easily conclude that, in the case where the fluorescence arising from FLA not included in the membrane is negligible, the total intensity of the fluorescence observed is the sum of the total fluorescence arising from each of the phases (see Fig. 5), which may be equated as

$$F_1^{\lambda_{em}} = \alpha\varepsilon_1^{\lambda_{ex}}[A_1]x_1 y_1^{\lambda_{em}}\Phi_1$$
$$F_2^{\lambda_{em}} = \alpha\varepsilon_2^{\lambda_{ex}}[A_2](1 - x_1)y_2^{\lambda_{em}}\Phi_2 \quad (14)$$

where α is a constant depending on the geometric characteristics of the experimental setup and sample. The value of $K_{P(L)}$ may be obtained from the ratio of the emission intensity of the same FLA concentration in a mixture of phases, I, to that in a pure phase, for example, phase 2, I_2, using Eq. (15):

$$\frac{I}{I_2} = 1 + \xi K_{P(L)} \frac{x_1}{1 - x_1} \quad (15)$$

Again, the experimental methodology is straightforward once the value of ξ is known, and choosing the excitation and emission wavelengths coincident with the isosbestic and isoemissive points greatly simplifies the task.

Spectral Distribution. The analysis for obtaining the concentrations in each coexistent membrane phase is straightforward, once the two emission spectra in the two pure phases are known for the same concentration of FLA.

EXPERIMENTAL RESULTS ON FLA PARTITIONING BETWEEN PHASES IN MODEL SYSTEMS

In Table I we have compiled some of the available data on fluorescent probe partitioning between membrane lipid phases. Only data that have a numerical value for $K_{P(L)}$ are included in the table. Most of the information available in the literature in this regard has to do with the partitioning of FLA between solid or gel (s) and liquid-disordered (l_d) phases, and a very small fraction concerns partitioning between liquid-ordered (l_o) and l_d phases. No information is available for $K_{P(L)}$ between s and l_o phases. Phase separations of the l_o/l_d type or even of the type in which two immiscible l_o phases coexist in the same membrane may, however, be the most biologically relevant form of membrane heterogeneity and include "raft" domains. However, since knowledge of $K_{P(L)}$ is essential for the eventual application of quantitative microscopy to inhomogeneities in cell plasma membranes, we review the reported work due to its methodological value.

In terms of methodology, two fundamentally different approaches to the determination of $K_{P(L)}$ are possible: (1) $K_{P(L)}$ can be determined directly for partitioning between two phases that coexist in the same lipid bilayer membrane; and (2) $K_{P(L)}$ can be determined indirectly by one of two methods—(a) by quantifying the distribution, at equilibrium, of an FLA between two populations of lipid vesicles (or other form of bilayer membranes), each of which represents one of the phases to be studied or (b) by measuring K_P, the lipid-phase/aqueous-phase partition coefficient, for each of the lipid phases independently (K_{P1}, K_{P2}) and using the expression

$$K_{P(L)} = \frac{K_{P1}}{K_{P2}} \quad (16)$$

All of these approaches have been used in the literature; all have some advantages and some disadvantages. Since $K_{P(L)}$ is an equilibrium thermodynamic quantity, it is necessary to ensure that the system on which a measurement is being made is at equilibrium. Direct determination of $K_{P(L)}$ leaves no ambiguity about the identities of the phases that do in fact coexist in the membrane of interest but requires the availability of good phase diagrams for estimation of the mass (or molar) fractions of coexisting membrane phases. The indirect methods are experimentally simpler to execute but require that some precautions be taken. In the equilibration of FLA between two membrane vesicle populations, for example, care must be taken to ensure that there is no mixing of components of the two membrane populations other than the FLA whose behavior is to be studied. This approach, therefore, excludes studies on FLAs whose K_P very strongly favors the lipid phase compared to the aqueous phase since the exchange of these molecules between the two vesicle populations is likely to be very slow, if not just as slow as the exchange of host membrane lipid components themselves. In studying the partitioning of FLA between an aqueous phase and a lipid membrane phase, the existence of micellar aggregates or other form of aggregates in the system at equilibrium also may not be ignored.

Three methods have dominated in the determinations of $K_{P(L)}$ reported in the literature for membrane phases that coexist with each other in the same lipid bilayer: (1) steady-state fluorescence emission intensity or quantum yield determination; (2) steady-state fluorescence polarization or anisotropy measurements, and (3) static quenching of FLA fluorescence. In the "indirect" measurement of $K_{P(L)}$, i.e., by separate measurement of K_P between the individual lipid phases and the aqueous phase or by measurement of the equilibrium partitioning of an FLA between the two phases existent as separate populations of lipid vesicles, difference absorption spectroscopy between FLA in the aqueous phase and FLA in the membrane-bound state [59] and direct measurements of insertion and desorption rate constants of an FLA monomer into/from a membrane surface from/to an aqueous phase [47] have been used.

Table I. Summary of the Partition Coefficients ($K_{P(L)}$) Reported in the Literature for the Partitioning of Fluorescent Lipid Amphiphiles Between two Lipid Phases[a,b]

Probe	Ref.[c]	Host phase	Type	T (°C)[d]	Method of determination	$K_{P(L)}$
Perylene	1	$DiC_{18:0}PC/diC_{16:0}PC$	s/l_d		Fluorescence emission intensity	~1
	1	$DiC_{16:0}PE/diC_{16:0}PC$	s/l_d		Fluorescence emission intensity	~1
DPH	2	$DiC_{16:0}PC/diC_{14:0}PC$	s/l_d	28	Steady-state fluorescence anisotropy (equilibrium partitioning between pure phase liposomes)	0.97 ± 0.04 1.04 ± 0.04
	3	$DiC_{16:0}PC$/SL-PC	s/l_d	23	Fluorescence quenching	0.5–1
	4	$Ca(diC_{18:1}PS)_2$/SL–PC (excess Ca^{2+})[e]	s'/l_d	26	Fluorescence quenching	0.08 ± 0.01
	5	Egg PC/SL–PA (excess Cd^{2+})	s'/l_d	(a)	Fluorescence quenching	1
	6	$DiC_{16:0}PC$/SL–PC[e]	s/l_d	25	Fluorescence quenching	0.67 ± 0.22
	6	$DiC_{18:0}PC$/SL–PC[e]	s/l_d	25	Fluorescence quenching	0.67 ± 0.22
	7	$DiC_{18:0}PC/diC_{14:0}PC$	s/l_d	32–44 (b)	Steady-state fluorescence anisotropy	0.303
TMA–DPH	7	$DiC_{16:0}PC/diC_{14:0}PC$	s/l_d	(a)	Steady-state fluorescence polarization (equilibrium partitioning between pure phase liposomes)	0.313
*t*PnA	8	$DiC_{16:0}PC/C_{16:0}C_{22:6}PC$	s/l_d	22	Absorption spectroscopy (derived from lipid-phase/aqueous-phase partitions)	2.9 ± 0.7
	8	$DiC_{16:0}PC/C_{16:0}C_{22:6}PC$	s/l_d	(a)	Steady-state fluorescence polarization	5.1 ± 1.2
	8	$DiC_{16:0}PC/C_{16:0}C_{22:6}PC$	s/l_d	(a)	Fluorescence emission quantum yield	3.4 ± 0.7
	9	$DiC_{16:0}PC/C_{16:0}C_{22:6}PC$	s/l_d	(b)	Steady-state fluorescence polarization	4.9 ± 2.3
	9	$DiC_{16:0}PC/C_{16:0}C_{22:6}PC$	s/l_d	(b)	Fluorescence emission quantum yield	6.3 ± 4.1
	4	$Ca(diC_{18:1}PS)_2$/SL–PC (excess Ca^{2+})[e]	s'/l_d	26	Fluorescence quenching	0.33 ± 0.11
	10	$DiC_{16:0}PC/C_{16:0}C_{22:6}PC$		(b)	Steady-state fluorescence polarization	5.2 ± 1.9
	10	$DiC_{16:0}PC/C_{16:0}C_{22:6}PC$		(b)	Fluorescence emission quantum yield	5.8 ± 3.0
*c*PnA	8	$DiC_{16:0}PC/C_{16:0}C_{22:6}PC$	s/l_d	22	Absorption spectroscopy (derived from lipid-phase/aqueous-phase partitions)	0.6 ± 0.2
	8	$DiC_{16:0}PC/C_{16:0}C_{22:6}PC$	s/l_d	(a)	Steady-state fluorescence polarization	0.6 ± 0.1
	8	$DiC_{16:0}PC/C_{16:0}C_{22:6}PC$	s/l_d	(a)	Fluorescence emission quantum yield	0.8 ± 0.3
	9	$DiC_{16:0}PC/C_{16:0}C_{22:6}PC$	s/l_d	(b)	Steady-state fluorescence polarization	0.7 ± 0.9
	9	$DiC_{16:0}PC/C_{16:0}C_{22:6}PC$	s/l_d	(b)	Fluorescence emission quantum yield	0.5 ± 0.2
	10	$DiC_{16:0}PC/C_{16:0}C_{22:6}PC$	s/l_d	(b)	Steady-state fluorescence polarization	0.70 ± 0.18
	10	$DiC_{16:0}PC/C_{16:0}C_{22:6}PC$	s/l_d	(b)	Fluorescence emission quantum yield	0.65 ± 0.19
$1\text{-}C_{16:0}$–2-*t*PnA PC	9	$DiC_{16:0}PC/C_{16:0}C_{22:6}PC$	s/l_d	(b)	Steady-state fluorescence polarization	4.3 ± 2.4
	9	$DiC_{16:0}PC/C_{16:0}C_{22:6}PC$	s/l_d	(b)	Fluorescence emission quantum yield	10.0 ± 6.4
$1\text{-}C_{18:1}$–2-*t*PnA PC	9	$DiC_{16:0}PC/C_{16:0}C_{22:6}PC$	s/l_d	(b)	Steady-state fluorescence polarization	0.6 ± 0.3
	9	$DiC_{16:0}PC/C_{16:0}C_{22:6}PC$	s/l_d	(b)	Fluorescence emission quantum yield	0.7 ± 0.3
$1\text{-}C_{16:0}$–2-*t*PnA PE	9	$DiC_{16:0}PC/C_{16:0}C_{22:6}PC$	s/l_d	(b)	Steady-state fluorescence polarization	5.0 ± 2.5
	9	$DiC_{16:0}PC/C_{16:0}C_{22:6}PC$	s/l_d	(b)	Fluorescence emission quantum yield	13.8 ± 6.9
	11	$DiC_{16:0}PC/diC_{18:2}PC$	s/l_d	(b)	Steady-state fluorescence polarization	4.5 ± 1.4
	11	$DiC_{16:0}PC/diC_{18:2}PC$	s/l_d	(b)	Fluorescence emission quantum yield	3.4 ± 1.5
$1\text{-}C_{16:0}$–2-*t*PnA PG	11	$DiC_{16:0}PC/diC_{18:2}PC$	s/l_d	(b)	Steady-state fluorescence polarization	7.2 ± 14.0
	11	$DiC_{16:0}PC/diC_{18:2}PC$	s/l_d	(b)	Fluorescence emission quantum yield	2.1 ± 0.7
$1\text{-}C_{18:1}$–2-*t*PnA PE	9	$DiC_{16:0}PC/C_{16:0}C_{22:6}PC$	s/l_d	(b)	Steady-state fluorescence polarization	0.6 ± 0.4
	9	$DPPC/C_{16:0}C_{22:6}PC$	s/l_d	(b)	Fluorescence emission quantum yield	0.8 ± 0.2
N-*t*PnA glucosylcerebroside	10	$DiC_{16:0}PC/C_{16:0}C_{22:6}PC$	s/l_d	(b)	Steady-state fluorescence polarization	0.66 ± 0.08
	10	$DiC_{16:0}PC/C_{16:0}C_{22:6}PC$	s/l_d	(b)	Fluorescence emission quantum yield	0.72 ± 0.29
N-*t*PnA ceramide	10	$DiC_{16:0}PC/C_{16:0}C_{22:6}PC$	s/l_d	(b)	Steady-state fluorescence polarization	0.59 ± 0.40
	10	$DiC_{16:0}PC/C_{16:0}C_{22:6}PC$	s/l_d	(b)	Fluorescence emission quantum yield	0.45 ± 0.25
$1\text{-}C_{16:0}$–2-*c*PnA PC	9	$DiC_{16:0}PC/C_{16:0}C_{22:6}PC$	s/l_d	(b)	Steady-state fluorescence polarization	0.6 ± 0.3
	9	$DiC_{16:0}PC/C_{16:0}C_{22:6}PC$	s/l_d	(b)	Fluorescence emission quantum yield	0.6 ± 0.2
	10	$DiC_{16:0}PC/C_{16:0}C_{22:6}PC$	s/l_d	(b)	Steady-state fluorescence polarization	0.70 ± 0.40

Table I—*Continued.*

Probe	Ref.[c]	Host phase	Type	T (°C)[d]	Method of determination	$K_{P(L)}$
	10	$DiC_{16:0}PC/C_{16:0}C_{22:6}PC$	s/l_d	(b)	Fluorescence emission quantum yield	0.63 ± 0.19
1-$C_{18:1}$–2-*c*PnA PC	9	$DiC_{16:0}PC/C_{16:0}C_{22:6}PC$	s/l_d	(b)	Steady-state fluorescence polarization	0.3 ± 0.1
	9	$DiC_{16:0}PC/C_{16:0}C_{22:6}PC$	s/l_d	(b)	Fluorescence emission quantum yield	0.2 ± 0.1
1-$C_{16:0}$–2-*c*PnA PE	9	$DiC_{16:0}PC/C_{16:0}C_{22:6}PC$	s/l_d	(b)	Steady-state fluorescence polarization	1.0 ± 0.4
	9	$DiC_{16:0}PC/C_{16:0}C_{22:6}PC$	s/l_d	(b)	Fluorescence emission quantum yield	1.0 ± 0.2
1-$C_{18:1}$–2-*c*PnA PE	9	$DiC_{16:0}PC/C_{16:0}C_{22:6}PC$	s/l_d	(b)	Steady-state fluorescence polarization	0.4 ± 0.4
	9	$DiC_{16:0}PC/C_{16:0}C_{22:6}PC$	s/l_d	(b)	Fluorescence emission quantum yield	0.5 ± 0.5
	11	$DiC_{16:0}PC/diC_{18:2}PC$	s/l_d	(b)	Steady-state fluorescence polarization	0.13 ± 0.03
	11	$DiC_{16:0}PC/diC_{18:2}PC$	s/l_d	(b)	Fluorescence emission quantum yield	0.4 ± 0.3
1-$C_{18:1}$–2-*c*PnA PG	11	$DiC_{16:0}PC/diC_{18:2}PC$	s/l_d	(b)	Steady-state fluorescence polarization	0.3 ± 0.1
	11	$DiC_{16:0}PC/diC_{18:2}PC$	s/l_d	(b)	Fluorescence emission quantum yield	0.2 ± 0.1
1-$C_{18:1}$–2-*t*PnA PC	12	$DiC_{16:0}PC/diC_{18:2}PC$	s/l_d	(b)	Steady-state fluorescence polarization	0.4 ± 0.1
	12	$DiC_{16:0}PC/diC_{18:2}PC$	s/l_d	(b)	Fluorescence emission quantum yield	0.9 ± 0.2
1-$C_{18:1}$–2-*t*PnA PE	12	$DiC_{16:0}PC/diC_{18:2}PC$	s/l_d	(b)	Steady-state fluorescence polarization	0.6 ± 0.6
	12	$DiC_{16:0}PC/diC_{18:2}PC$	s/l_d	(b)	Fluorescence emission quantum yield	1.2 ± 0.5
1-$C_{16:0}$–2-*c*PnA PC	12	$DiC_{16:0}PC/diC_{18:2}PC$	s/l_d	(b)	Steady-state fluorescence polarization	0.6 ± 0.2
	12	$DiC_{16:0}PC/diC_{18:2}PC$	s/l_d	(b)	Fluorescence emission quantum yield	1.2 ± 0.4
1-$C_{16:0}$–2-*c*PnA PE	12	$DiC_{16:0}PC/diC_{18:2}PC$	s/l_d	(b)	Steady-state fluorescence polarization	0.8 ± 0.3
	12	$DiC_{16:0}PC/diC_{18:2}PC$	s/l_d	(b)	Fluorescence emission quantum yield	1.6 ± 0.3
t-COPA	13	$DiC_{14:0}PC$ (s and l_d phases examined independently)	s/l_d	(c)	Fluorescence emission quantum yield (derived from lipid-phase/aqueous-phase partitions)	1.4 ± 0.4
c-COPA	13	$DiC_{14:0}PC$ (s and l_d phases examined independently)	s/l_d	(c)	Fluorescence emission quantum yield (derived from lipid-phase/aqueous-phase partitions)	1.4 ± 0.4
1-$C_{16:0}$–2-DNS–$C_{11:0}$ PE	14	$DiC_{16:0}PC/diC_{18:2}PC$	s/l_d	(b)	Steady-state fluorescence polarization	0.08 ± 0.03
1-$C_{18:1}$–2-DNS–$C_{4:0}$ PE	14	$DiC_{16:0}PC/diC_{18:2}PC$	s/l_d	(b)	Steady-state fluorescence polarization	0.2 ± 0.1
Prodan	15	$DiC_{16:0}PC/diC_{12:0}PC$	s/l_d	25	Fluorescence emission intensity (derived from lipid-phase/aqueous-phase partitions)	0.03
3-(9-Anthroyloxy) stearic acid	6	$DiC_{16:0}PC$/SL–PC[e]	s/l_d	25	Fluorescence quenching	0.4 ± 0.08
	6	$DiC_{18:0}PC$/SL–PC[e]	s/l_d	25	Fluorescence quenching	0.25 ± 0.06
	6	$Ca(diC_{18:1}PS)_2$/SL–PC (excess Ca^{2+})[e]	s/l_d	25	Fluorescence quenching	0.06 ± 0.01
6-(9-Anthroyloxy)stearic acid	6	$DiC_{16:0}PC$/SL–PC[e]	s/l_d	25	Fluorescence quenching	0.25 ± 0.06
	6	$DiC_{18:0}PC$/SL–PC[e]	s/l_d	25	Fluorescence quenching	0.20 ± 0.12
	6	$Ca(diC_{18:1}PS)_2$/SL–PC (excess Ca^{2+})[e]	s/l_d	25	Fluorescence quenching	0.06 ± 0.01
9-(9-Anthroyloxy)stearic acid	6	$DiC_{16:0}PC$/SL–PC[e]	s/l_d	25	Fluorescence quenching	0.25 ± 0.06
	6	$DiC_{18:0}PC$/SL–PC[e]	s/l_d	25	Fluorescence quenching	0.25 ± 0.13
	6	$Ca(diC_{18:1}PS)_2$/SL–PC (excess Ca^{2+})[e]	s/l_d	25	Fluorescence quenching	0.06 ± 0.01
12-(9-Anthroyloxy)stearic acid	6	$DiC_{16:0}PC$/SL–PC[e]	s/l_d	25	Fluorescence quenching	0.25 ± 0.06
	6	$DiC_{18:0}PC$/SL–PC[e]	s/l_d	25	Fluorescence quenching	0.17 ± 0.08
	6	$Ca(diC_{18:1}PS)_2$/SL–PC (excess Ca^{2+})[e]	s/l_d	25	Fluorescence quenching	0.05 ± 0.01
	16	$DiC_{16:0}PC/diC_{12:0}PC$	s/l_d		Fluorescence polarization	~0

Table I—*Continued.*

Probe	Ref.[c]	Host phase	Type	T (°C)[d]	Method of determination	$K_{P(L)}$
12-(9-Anthroyloxy) stearic acid methyl ester	4	$Ca(diC_{18:1}PS)_2$/SL–PC (excess Ca^{2+})[e]	s'/l_d	26	Fluorescence quenching	0.06 ± 0.01
11-(9-Anthroyloxy)undecanoic acid	6	$DiC_{16:0}PC$/SL–PC[e]	s/l_d	25	Fluorescence quenching	0.25 ± 0.06
	6	$DiC_{18:0}PC$/SL–PC[e]	s/l_d	25	Fluorescence quenching	0.20 ± 0.08
	6	$Ca(diC_{18:1}PS)_2$/SL–PC (excess Ca^{2+})[e]	s'/l_d	25	Fluorescence quenching	0.06 ± 0.01
16-(9-Anthroyloxy)palmitic acid	6	$DiC_{16:0}PC$/SL–PC[e]	s/l_d	25	Fluorescence quenching	0.67 ± 0.22
	6	$DiC_{18:0}PC$/SL–PC[e]	s/l_d	25	Fluorescence quenching	0.67 ± 0.22
	6	$Ca(diC_{18:1}PS)_2$/SL–PC (excess Ca^{2+})[e]	s'/l_d	25	Fluorescence quenching	0.08 ± 0.01
1-Acyl-2-[12-(9-Anthroyloxy)stearoyl] PC	4	$Ca(diC_{18:1}PS)_2$/SL–PC (excess Ca^{2+})[e]	s'/l_d	26	Fluorescence quenching	0.01 ± 0.002
1-Acyl-2-[12-(9-Anthroyloxy)stearoyl] PS	4	$Ca(diC_{18:1}PS)_2$/SL–PC (excess Ca^{2+})[e]	s'/l_d	26	Fluorescence quenching	1.0 ± 0.02
$C_{12:0}$DiI	17	$DiC_{18:0}PC$/SL–PC	s/l_d	21	Fluorescence quenching	0.17 ± 0.01
	17	$DiC_{16:0}PC$/SL–PC	s/l_d	21	Fluorescence quenching	1.25 ± 0.16
	17	$Ca(diC_{18:1}PS)_2$/SL–PC (excess Ca^{2+})[e]	s'/l_d	21	Fluorescence quenching	0.13 ± 0.01
$C_{16:0}$DiI	17	$DiC_{18:0}PC$/SL–PC	s/l_d	21	Fluorescence quenching	0.56 ± 0.09
	17	$DiC_{18:0}PC$/SL–PC	s/l_d	35	Fluorescence quenching	0.67 ± 0.13
	17	$DiC_{16:0}PC$/SL–PC	s/l_d	21	Fluorescence quenching	2.0 ± 0.4
	17	$Ca(diC_{18:1}PS)_2$/SL–PC (excess Ca^{2+})[e]	s'/l_d	21	Fluorescence quenching	0.17 ± 0.01
$C_{18:0}$DiI	17	$DiC_{18:0}PC$/SL–PC	s/l_d	21	Fluorescence quenching	11.1 ± 1.2
	17	$DiC_{18:0}PC$/SL–PC	s/l_d	35	Fluorescence quenching	2.5 ± 0.6
	17	$DiC_{16:0}PC$/SL–PC	s/l_d	21	Fluorescence quenching	2.9 ± 0.4
	17	$Ca(diC_{18:1}PS)_2$/SL–PC (excess Ca^{2+})[e]	s'/l_d	21	Fluorescence quenching	0.20 ± 0.03
$C_{20:0}$DiI	17	$DiC_{18:0}PC$/SL–PC	s/l_d	21	Fluorescence quenching	50 ± 25
	17	$DiC_{18:0}PC$/SL–PC	s/l_d	35	Fluorescence quenching	6.7 ± 2.7
	17	$DiC_{16:0}PC$/SL–PC	s/l_d	21	Fluorescence quenching	4.0 ± 0.8
	17	$Ca(diC_{18:1}PS)_2$/SL–PC (excess Ca^{2+})[e]	s'/l_d	21	Fluorescence quenching	0.28 ± 0.04
$C_{22:0}$DiI	17	$DiC_{18:0}PC$/SL–PC	s/l_d	21	Fluorescence quenching	25 ± 6
	17	$DiC_{18:0}PC$/SL–PC	s/l_d	35	Fluorescence quenching	5.0 ± 1.3
	17	$DiC_{16:0}PC$/SL–PC	s/l_d	21	Fluorescence quenching	1.4 ± 0.2
	17	$Ca(diC_{18:1}PS)_2$/SL–PC (excess Ca^{2+})[e]	s'/l_d	21	Fluorescence quenching	0.22 ± 0.02
NBD–$C_{12:0}$	18	$DiC_{18:0}PC/diC_{12:0}PC$	s/l_d	20	Steady-state fluorescence emission anisotropy	0.2 (h)/0.5 (c)[f]
	18	$DiC_{18:0}PC/diC_{12:0}PC$	s/l_d	30	Steady-state fluorescence emission anisotropy	0.2 (h)/0.6 (c)
NBD–$C_{14:0}$	18	$DiC_{18:0}PC/diC_{12:0}PC$	s/l_d	20	Steady-state fluorescence emission anisotropy	0.5 (h)/0.6 (c)
	18	$DiC_{18:0}PC/diC_{12:0}PC$	s/l_d	30	Steady-state fluorescence emission anisotropy	0.6 (h)/0.7 (c)
NBD–$C_{16:0}$	18	$DiC_{18:0}PC/diC_{12:0}PC$	s/l_d	20	Steady-state fluorescence emission anisotropy	1.0 (h)/0.9 (c)
	18	$DiC_{18:0}PC/diC_{12:0}PC$	s/l_d	30	Steady-state fluorescence emission anisotropy	1.3 (h)/1.3 (c)
NBD–$C_{18:0}$	18	$DiC_{18:0}PC/diC_{12:0}PC$	s/l_d	20	Steady-state fluorescence emission anisotropy	1.7 (h)/1.5 (c)
	18	$DiC_{18:0}PC/diC_{12:0}PC$	s/l_d	30	Steady-state fluorescence emission anisotropy	2.5 (h)/1.7 (c)
NBD–$C_{18:1}$	18	$DiC_{18:0}PC/diC_{12:0}PC$	s/l_d	20	Steady-state fluorescence emission anisotropy	0.1 (h)/0.5 (c)

Table I—*Continued.*

Probe	Ref.[c]	Host phase	Type	T (°C)[d]	Method of determination	$K_{P(L)}$
	18	$DiC_{18:0}PC/diC_{12:0}PC$	s/l_d	30	Steady-state fluorescence emission anisotropy	0.4 (h)/0.6 (c)
NBD–$diC_{12:0}PE$	18	$DiC_{18:0}PC/diC_{12:0}PC$	s/l_d	20	Steady-state fluorescence emission anisotropy	0.0 (h)/0.0 (c)
	18	$DiC_{18:0}PC/diC_{12:0}PC$	s/l_d	30	Steady-state fluorescence emission anisotropy	0.0 (h)/0.0 (c)
	19	$DiC_{12:0}PC/C_{22:1(\Delta13)}C_{22:1(\Delta13)}PC$	l_d/l_d	40	Equilibrium probe exchange between vesicle populations	1.4
	19	$C_{16:0}C_{18:1(\Delta9)}PC/C_{22:1(\Delta13)}C_{22:1(\Delta13)}PC$	l_d/l_d	40	Equilibrium probe exchange between vesicle populations	1.2
	19	$C_{16:1(\Delta9)}C_{16:1(\Delta9)}PC/C_{22:1(\Delta13)}C_{22:1(\Delta13)}PC$	l_d/l_d	40	Equilibrium probe exchange between vesicle populations	1.8
	19	$C_{18:1(\Delta9)}C_{18:1(\Delta9)}PC/C_{22:1(\Delta13)}C_{22:1(\Delta13)}PC$	l_d/l_d	40	Equilibrium probe exchange between vesicle populations	1.4
	19	$C_{18:1(\Delta6)}C_{18:1(\Delta6)}PC/C_{22:1(\Delta13)}C_{22:1(\Delta13)}PC$	l_d/l_d	40	Equilibrium probe exchange between vesicle populations	1.6
	19	$C_{20:1(\Delta11)}C_{20:1(\Delta11)}PC/C_{22:1(\Delta13)}C_{22:1(\Delta13)}PC$	l_d/l_d	40	Equilibrium probe exchange between vesicle populations	1.4
	19	$C_{16:0}C_{18:1(\Delta9)}PS/C_{18:1(\Delta9)}C_{18:1(\Delta9)}PS$	l_d/l_d	40	Equilibrium probe exchange between vesicle populations	1.2
	19	$C_{16:0}C_{18:1(\Delta9)}PG/C_{18:1(\Delta9)}C_{18:1(\Delta9)}PG$	l_d/l_d	40	Equilibrium probe exchange between vesicle populations	1.10 ± 0.02
NBD–$diC_{14:0}PE$	18	$DiC_{18:0}PC/diC_{12:0}PC$	s/l_d	20	Steady-state fluorescence emission anisotropy	0.4 (h)/0.5 (c)
	18	$DiC_{18:0}PC/diC_{12:0}PC$	s/l_d	30	Steady-state fluorescence emission anisotropy	0.5 (h)/0.5 (c)
	20	$DiC_{14:0}PC$/cholesterol	l_o/l_d	30	Steady-state fluorescence anisotropy	1.1
	20	$DiC_{14:0}PC$/cholesterol	l_o/l_d	40	Steady-state fluorescence anisotropy	2.6
NBD–$diC_{16:0}PE$	18	$DiC_{18:0}PC/diC_{12:0}PC$	s/l_d	20	Steady-state fluorescence emission anisotropy	1.0 (h)/1.1 (c)
	18	$DiC_{18:0}PC/diC_{12:0}PC$	s/l_d	30	Steady-state fluorescence emission anisotropy	1.1 (h)/1.2 (c)
NBD–$diC_{18:0}PE$	18	$DiC_{18:0}PC/diC_{12:0}PC$	s/l_d	20	Steady-state fluorescence emission anisotropy	1.0 (h)/1.1 (c)
	18	$DiC_{18:0}PC/diC_{12:0}PC$	s/l_d	30	Steady-state fluorescence emission anisotropy	1.3 (h)/1.4 (c)
	18	$DiC_{14:0}PC$/cholesterol	l_o/l_d	30	Steady-state fluorescence emission anisotropy	1.0 ± 0.4
NBD–$C_{16:0}C_{18:1}PE$	18	$DiC_{18:0}PC/diC_{12:0}PC$	s/l_d	20	Steady-state fluorescence emission anisotropy	0.0 (h)/0.0 (c)
	18	$DiC_{18:0}PC/diC_{12:0}PC$	s/l_d	30	Steady-state fluorescence emission anisotropy	0.0 (h)/0.1 (c)
	18	$DiC_{14:0}PC$/cholesterol	l_o/l_d		Steady-state fluorescence emission anisotropy	0.4 ± 0.1
U-6	21	$DiC_{14:0}PC/diC_{14:0}PC$–cholesterol (65/35)	l_o/l_d		Values obtained from kinetics of probe insertion into bilayers	0.21
N-(Lissamine–rhodamine B) $diC_{14:0}PE$	20	$DiC_{14:0}PC$/cholesterol	l_o/l_d	30	Excited-state lifetime and steady-state fluorescence intensity	0.30
	20	$DiC_{14:0}PC$/cholesterol	l_o/l_d	40	Excited-state lifetime and steady-state fluorescence intensity	0.27

[a] For a list of abbreviations please see the Appendix.

[b] $K_{P(L)}$ is always given for partition between a more ordered (solid, liquid-ordered) and a less ordered (liquid-ordered, liquid-disordered) phase, i.e., $K_{P(L)} = [A_1]/[A_2]$; see Eq. (4) in text.

[c] (1) Ref. 17; (2) Ref. 31; (3) Ref. 33; (4) Ref. 16; (5) Ref. 14; (6) Ref. 22; (7) Ref. 46; (8) Ref. 59; (9) Ref. 76; (10) Ref. 51; (11) Ref. 38; (12) Ref. 75; (13) Ref. 39; (14) Ref. 6; (15) Ref. 30; (16) Ref. 7; (17) Ref. 61; (18) Ref. 41; (19) Ref. 15; (20) Ref. 35; (21) Ref. 47.

Table I—*Continued.*

[d] (a) Temperature not specified. (b) Data were averaged over a wide range of temperatures. (c) K_P was measured independently at different temperatures for partitioning of the FLA between pure lipid phases and an aqueous phase, and the values of K_P obtained, at different temperatures, were used to calculate $K_{P(L)}$.

[e] The authors have preferred to report a "concentration ratio" instead of a $K_{P(L)}$ in these cases, arguing that slow diffusional redistribution of the fluorescent amphiphile probe "trapped" in the gel or other solid phase may cause the system not to be at equilibrium. This concentration ratio is identical to $K_{P(L)}$ at equilibrium. The preoccupation may be especially justified in the case of systems that have a $Ca(PS)_2$-rich solid phase, which may be dehydrated and considerably more highly ordered than a typical hydrated, thermotropically induced gel phase. This phase is referred to as the s' phase in the table. For further details see Ref. 16 and the discussion of this phase structure therein.

[f] Values are reported for heating (h) and cooling (c) scans.

FLA exchange between two lipid vesicle populations of distinct phase properties, in one population of which a nontransferable quencher has been included [42,43], have been used to study the equilibrium exchange between phases of rapidly exchanging FLAs derived from phosphoglycero- or sphingolipids [15,18,53,54,72]. These rapidly exchanging FLAs are either short-chain lipids or lipids in which one of the apolar chains was substituted by a fluorescent derivative whose charge or polarity forced this chain to expose the fluorophore to the bilayer–water interface [12]. In the present context the results of this work are of interest due to the demonstration that FLA partitioning is not necessarily identical for all phases of the same designation [for example, l_d phases (see Ref. 15) and charged *versus* neutral membrane surfaces (see Ref. 18)] and the fact that small but significant differences in partition behavior (within a factor of two- to three fold) may result from differences in probe headgroup characteristics [18].

Fluorescence emission intensity or quantum yields can be different for FLAs in different phases, be they lipid or aqueous. These differences in emission intensities (quantum yields) have been exploited in some of the earliest work in this field that studied the partition of *trans*- and *cis*-parinaric acids [59] and perylene [17] between coexisting *s* and l_d membrane phases. The method developed by Sklar and co-workers was later used by Welti and co-workers [38,75,76] to study the partition of several phospholipid derivatives that included *trans*- and *cis*-parinaric acid in their structure and by Rintoul *et al.*[51] to study the partition of *N-trans*-parinaroylsphingosine (ceramide) and *N-trans*-parinaroylglucosylcerebroside between coexistent *s* and l_d phases.

Steady-state fluorescence anisotropy (polarization) was used in the first determination of the equilibrium partitioning of a fluorophore (DPH) between *s*-phase $diC_{18:0}PC$ and l_d-phase $diC_{14:0}PC$ liposomes by Lentz *et al.*[31]. Its use was then extended to the study of *trans*- and *cis*-parinaric acid partitioning between *s* and l_d fluid phases by Sklar *et al.* [59] and applied to the partitioning of several glycerophospholipid and sphingolipid derivatives of *trans*- and *cis*-parinaric acids between these phases by Welti and co-workers and by Rintoul *et al.* Partitioning of the probes occurred between an *s* phase rich in $diC_{16:0}PC$ and an l_d phase rich in $C_{16:0}C_{22:6}PC$ coexistent in the same lipid bilayer. In these studies, $K_{P(L)}$ values obtained for the same system using fluorescence intensity/quantum yield measurements and steady-state fluorescence polarization measurements were shown to be comparable. Steady-state polarization of fluorescence was also used in a recent study [41] of the partitioning of a homologous series of NBD–amino alkanes and NBD–PEs, of varying chain lengths (between $C_{12:0}$ and $C_{18:0}$) and degrees of saturation ($C_{18:0}$ and $C_{18:1(\Delta^9 cis)}$), between coexisting *s* and l_d phases in lipid bilayers prepared from a mixture of $diC_{12:0}PC$ and $diC_{18:0}PC$. This study was extended to membranes made from a binary mixture of $diC_{14:0}PC$ and cholesterol with a coexistence of l_d and l_o phases in which the partitioning of NBD–$diC_{18:0}PE$ and NBD–$C_{18:1(\Delta^9 cis)}$)PC was examined. A similar study using NBD-$diC_{14:0}PC$ was reported by Loura *et al.* [35].

A third widely used method for determination of the $K_{P(L)}$ for FLA partitioning between coexistent *s* and l_d membrane phases is the quenching of fluorescence of the FLA by a spin-labeled phospholipid [32] or a phospholipid with a brominated acyl chain [55] which is the principal chemical constituent of the l_d phase. If the concentration of the quencher in the l_d phase is very high, static quenching of the FLA fluorescence may result. Feigenson and co-workers [14,16,22,32,33,61] have used this method to study the partition of a series of FLAs between *s* phases constituted primarily of saturated-chain PCs (in which the phase is thermally induced), or divalent metal ion-induced $diC_{18:1cis}PS$ solid phases, and a spin-labeled PC-rich l_d phase. A drawback of this method is that one of the phases, usually the l_d phase, has to be composed almost totally of the spin-labeled phospholipid derivative. Although it has been shown that this derivative forms hydrated lipid bilayers and vesicles [32], little else is known about the physical characteristics of this phase, and in any case, its relevance to phases that may exist

in biological systems is debatable. The partition behaviors of a homologous series of (9-anthroyloxy)-fatty acids with the anthroyloxy group located at various positions in the fatty acid chain [22] and a homologous series of dialkyl indocarbocynanines with saturated alkyl chain lengths of between 12 and 18 carbon atoms [61] between *s* and l_d phases rich in the spin-labeled phospholipid are summarized in Table I. Silvius and co-workers [72,73] have used the spin-labeled quencher approach to study the comparative partitioning of several FLAs between coexisting phases in lipid bilayers made from ternary mixtures of phosphoglycero- or sphingolipids, a spin-labeled PC derivative, and cholesterol at a 0.33 mole fraction. At the high cholesterol content of the membranes it is probable that the spin-labeled PC-rich phase also contains an appreciable amount of cholesterol. The phase coexistence in the bilayers studied is presented by the authors as being of the l_o/l_d type but this has, in our judgment, not been clearly demonstrated. In any case, it is probable that a saturated long-chain PC/cholesterol or sphingolipid/cholesterol l_o phase coexists in these systems with a spin-labeled PC-rich phase that also contains an appreciable amount of cholesterol and may be of the l_o or of the l_d type. This study is of particular interest since it is one of the first attempts in this sort of study to model the cell plasma membrane and "raft"-like phases. Two types of FLAs have been used: (1) headgroup-labeled FLAs, some derived from phosphatidylethanolamines [73]; and (2) acyl chain-modified modified FLAs derived from various phosphoglycero- and sphingolipids [72]. In the first set [73], the partitioning of the amphiphiles is reported as a relative value with a di-$C_{18:0}$ FLA having the identical headgroup. The general conclusion is that increasing the chain length increases the tendency to partition into a more ordered phase and increasing the unsaturation has the opposite effect. Low-temperature detergent (Triton X-100) solubilization of large unilamellar vesicles with one of the probes showed some correlation between the degree of "detergent insolubility" of the probe and its relative partitioning into a more ordered phase. The second set of experiments [72] reported the relative preference for a more ordered phase for a series of phosphoglycero- and sphingolipid derivatives in which the *sn*-2 acyl chain was replaced by a 3-(4-(6-phenyl-all-*trans*-1,3,5-hexatrienyl)phenyl)propanoyl- group. The reference derivative was a phosphatidylcholine with a tetradecanoyl chain in the *sn*-1 position. The general conclusion was that the effect of the headgroup structure on the partitioning behavior of the probes is small, the preference for more ordered phases being notably enhanced for glycosylceramide derivatives (by about a factor of 2) and reduced by having unsaturation in the *sn*-1 acyl chain.

Despite the large volume of data accumulated over the years concerning the partitioning of FLAs between coexistent lipid phases, there are relatively few general conclusions of predictive value that can be derived from it. It appears to be reasonably clear that FLA preference for a fluid phase has to do with the length of the apolar portion of the molecule and how well it "fits" into the lipid packing lattice. Thus long fully saturated chains favor partitioning into ordered phases (domains) and shorter chains have an increasing tendency to partition into less ordered phases (domains). Unsaturation of the *cis*- type in the apolar chains of the FLA makes them prefer disordered phases; the greater the amount of unsaturation, the greater the preference. Unsaturation of the *trans* type predisposes the FLA to prefer a more ordered phase, though this may not always be the case. Bulky fluorophores in the apolar portion of the FLA molecule are more or less indifferent to the host phase if they have an all-*trans* rigid configurations, are relatively apolar themselves, and/or are located sufficiently close to the bilayer midplane. Commonly used fluorescent lipid derivatives, such as NBD-PCs and Bodipy-PCs, that have bulky aromatic polar groups attached to their acyl chains prefer disordered phases. The FLA headgroup does not seem to play a major role in the behavior of the probes (within a factor of about 2 in the values of the $K_{P(L)}$), with a few notable exceptions. As would be expected, different phases of the same general description (*s*, l_o, or l_d) are not necessarily identical, partly as a consequence of the constituent lipid polar portions to participate or not in hydrogen bonding or as a consequence of the surface charge and sometimes because of the packing order in the *s* phase. The characteristics of the FLA (hydrogen bonding, charge of polar portion, nature of apolar portion) then play a role in its partition behavior. A serious deficiency in the available literature is the lack of information on the temperature dependence of partition behavior. Most reports do not specify the temperatures at which the studies were performed, others average results over a wide range of temperatures, and still others determine K_P for the partitioning of an FLA between an aqueous phase and lipid phases at widely different temperatures to obtain a value of $K_{P(L)}$ for partition between two phases. The latter two approaches are clearly physically wrong since K_P and $K_{P(L)}$ are temperature-dependent quantities. Detailed studies of the temperature dependence of $K_{P(L)}$ would permit conclusions about partition energetics which would have important predictive value.

APPENDIX

Abbreviations and Nomenclature

a_i	Amplitude of the *i*th component
A_L	Fluorescent lipid amphiphile in a membrane
A_W	Fluorescent lipid amphiphile in aqueous solution
C_A	Total concentration of a fluorescent lipid amphiphile
C_P	Total concentration of a lipid-binding protein
C_S	Surface concentration (moles/area) of a fluorescent lipid amphiphile in a membrane
$C_{n:x}$DiI	1,1′-Dialkyl-3,3,3′,3′-tetramethylindocarbocyanine in which the alkyl groups have *n* carbon atoms and *x* double bonds
$C_{x:y}$	*n*-Acyl or *n*-alkyl chains (considered to be *n*-acyl when referring to lipids) with *x* carbon atoms and *y* double bonds (considered to be of the *cis* configuration unless specified otherwise)
$C_{x:y}C_{x':y'}$	1-*n*-Acyl(*x*:*y*)-2-*n*-acyl(*x*′:*y*′) glycerolipids with *n*-acyl chains having *x* or *x*′ carbon atoms and *y* or *y*′ unsaturated bonds, respectively, in the *sn*-1 and *sn*-2 positions
1-$C_{18:0}$–2-DPH–PC	1-Octadecanoyl–2-[[2-[4-(6-phenylhexa-1,3,5-all-*trans*-trienyl)-phenyl]ethyl] carbonyl]–3-*sn*-glycerophosphocholine
c-COPA	Octadeca-8-*cis*-10,12,14,16-all-*trans*-pentaenoic acid
*c*PnA	Octadeca-9,11,13,15-*cis*,*trans*,*trans*, *cis*-tetraenoic acid or octadeca-9,11,13,15-*cis*,*trans*,-*trans*,*cis*-tetraenoyl-
DNS–$C_{4:0}$	5-*N*,*N*-Dimethylaminonaphthalenesulfonamido–4-butanoyl-
DNS–$C_{11:0}$	5-*N*,*N*-Dimethylamino naphthalenesulfonamido–11-undecanoyl-
DPH	1,6-Diphenylhexa-1,3,5-(all-*trans*)-triene;
$\varepsilon_t^{\lambda(ex)}$	Molar absorptivity of the *i*th component at the wavelength of excitation
Φ_i	Emission quantum yield of the *i*th component
f_i	Fraction of the total emission intensity originating from the phase *i*
$F(t)$	Time-dependent intensity of fluorescence
FLA	Fluorescent lipid amphiphile
$I_i^{\lambda(ex)}$	Number of quanta absorbed by the *i*th component at the wavelength of excitation
K_P	Equilibrium partition coefficient for partitioning between a membrane and an aqueous phase
$K_{P(L)}$	Equilibrium partition coefficient for partitioning between two membrane phases
k_{fi}	Radiative rate constant for the *i*th component
k_+, k_-	Reaction rate constants in the forward and reverse direction, respectively
λ_{em}, λ_{ex}	Fluorescence emission and excitation wavelengths
l_d	Liquid-disordered phase
l_o	Liquid-ordered phase
NBD	*N*-(7-Nitrobenzoxa-2,3-diazol-4-yl)
NBD–$C_{n:x}$	*N*-(7-Nitrobenzoxa-2,3-diazol-4-yl)–amino alkane in which the alkyl moiety has *n* carbon atoms and *x* double bonds with a *cis* configuration
NBD–$C_{n:x}C_{m:y}$PE	*N*-(7-Nitrobenzoxa-2,3-diazol-4-yl)–amino glycerophosphoethanolamine in which the acyl chain attached to the glycerol *sn*-1 position has *n* carbon atoms with *x* double bonds and the acyl group attached to the glycerol *sn*-1 position has *m* carbon atoms with *y* double bonds, both with a *cis* configuration

P	Lipid-binding protein
PA	Complex of a fluorescent lipid amphiphile bound to a lipid-binding protein
PC	1,2-Diacylglycerophosphocholine, or phosphatidylcholine
PE	1,2-Diacylglycerophosphoethanolamine, or phosphatidylethanolamine
PG	1,2-Diacylglycerophosphoglycerol, or phosphatidylglycerol
Prodan	6-Propionyl-2-dimethylaminonaphthalene
PS	1,2-Diacylglycerophosphoserine, or phosphatidylserine
r	Total fluorescence anisotropy
r_i	Fluorescence anisotropy of fluorophore A in phase i
r_0	Limiting anisotropy
S_L	Area of a membrane phase referred to the total volume of a reaction mixture
s	Solid or "gel" phase
s'	A solid or "gel" phase produced as a result of the interaction of a divalent metal cation (Ca^{2+} or Cd^{2+}) with a phosphatidylserine-rich bilayer or phase
SL–PC	1-Acyl-2-[2-(6-carboxyhexyl)-2-octyl-4,4-dimethyloxazolidinyl-3-oxyl]–*sn*-glycerophosphocholine
t	Time
TMA–DPH	1-[4(Trimethylammonio)phenyl]–6-phenylhexa-1,3,5-(all-*trans*)-triene
t-COPA	Octadeca-8,10,12,14,16-all-*trans*-pentaenoic acid
*t*PNA	Octadeca-9,11,13,15-all-*trans*-tetraenoic acid or Octadeca-9,11,13,15-all-*trans*-tetraenoyl-
τ_i	Excited-state lifetime of the ith component
U-6	4-(*N*,*N*-Dimethyl-*N*-tetradecyl ammonium)methyl-(7-hydroxycoumarin) chloride
v_+, v_-	Reaction rates in the forward and reverse direction, respectively
$y_i^{\lambda(em)}$	Fluorescence intensity of a fluorophore in phase i collected at λ_{em}/total fluorescence intensity of the fluorophore in phase i

ACKNOWLEDGMENTS

The work of the authors has been supported by the Portuguese Ministry for Science and Technology (MCT) through the Fundação para a Ciência e a Tecnologia (FCT) through the Praxis and Sapiens programs and by the Commission of the European Union through the Training and Mobility of Researchers (TMR) program. We thank Magda Abreu for permitting the use of her unpublished data.

REFERENCES

1. P. F. F. Almeida, W. L. C. Vaz and T. E. Thompson (1992) *Biochemistry* **31**, 6739–6747.
2. P. F. F. Almeida, W. L. C. Vaz and T.E. Thompson (1992) *Biochemistry* **31**, 7198–7210.
3. P. F. F. Almeida, W. L. C. Vaz and T. E. Thompson (1993) *Biophys. J.* **64**, 399–412.
4. T. Arvinte, A. Cudd, and K. Hildebrand (1986) *Biochim. Biophys. Acta* **860**, 215–228.
5. L. A. Bagatolli and E. Gratton (2000) *Biophys. J.* **78**, 290–305.
6. D. Bartlett, M. Glaser, and R. Welti (1997) *Biochim. Biophys. Acta* **1328**, 48–54.
7. C. L. Bashford, C. R. Morgan, and G. K. Radda (1976) *Biochim. Biophys. Acta* **426**, 157–172.
8. D. A. Brown and E. London (1998) *Annu. Rev. Cell Dev. Biol.* **14**, 111–136.
9. D. A. Brown and E. London (1998) *J. Membr. Biol.* **164**, 103–114.
10. D. A. Brown and E. London (2000) *J. Biol. Chem.* **275**, 17221–17224.
11. T. Bultmann, W. L. C. Vaz, E. C. C. Melo, R. B. Sisk and T. E. (1991) *Biochemistry* **30**, 5573–5579.
12. A. Chattopadhyay and E. London (1987) *Biochemistry* **26**, 39–45.
13. L. Davenport (1997) *Methods Enzymol.* **278**, 487–512.
14. G. W. Feigenson (1983) *Biochemistry* **22**, 3106–3112.
15. G. W. Feigenson (1997) *Biophys. J.* **73**, 3112–3121.
16. K. I. Florine and G. W. Feigenson (1987) *Biochemistry* **26**, 1757–1768.
17. M. C. Foster and J. Yguerabide (1979) *J. Membr. Biol.* **45**, 125–146.
18. M. A. Gardam, J. L. Itovich, and J. R. Silvius (1989) *Biochemistry* **28**, 884–893.
19. J. W. Gibbs (1873) *Trans. Conn. Acad.* **3**, 152–156.
20. M. C. Giocondi, V. Vié, E. Lesniewska, P. E. Milhiet, M. Zinke-Allmang, and C. Le Grimellec (2001) *Langmuir* **17**, 1653–1659.
21. C. W. Hollars and R. C. Dunn (1998) *Biophys. J.* **75**, 342–353.
22. N. Huang, K. Florine-Casteel, G. W. Feigenson, and C. Spink (1988) *Biochim. Biophys. Acta* **939**, 124–130.

23. J. Hwang, L. A. Gheber, L. Margolis, and M. Edidin (1998) *Biophys. J.* **74**, 2184–2190.
24. J. N. Israelachvilli (1977) *Biochim. Biophys. Acta* **469**, 221–225.
25. K. Jacobson and C. Dietrich (1999) *Trends Cell. Biol.* **9**, 87–91.
26. M. K. Jain (1983) R. C. Aloia (Ed.), *Membrane Fluidity in Biology, Vol. 1. Concepts of Membrane Structure*, Academic Press, New York, pp. 1–37.
27. M. K. Jain and H. B. White III (1977) In R. Paoletti and D. Kritchevsky (Eds.), *Advances in Lipid Research, Vol. 15*, Academic Press, New York, pp. 1–60.
28. R. D. Klausner and D. E. Wolf (1980) *Biochemistry* **19**, 6199–6203.
29. J. Korlach, P. Schwille, W. W. Webb and G. W. Feigenson (1999) *Proc. Natl. Acad. Sci USA* **96**, 8461–8466.
30. E. K. Krasnowska, E. Gratton and T. Parasassi (1998) *Biophys. J.* **74**, 1984–1993.
31. B. R. Lentz, Y. Barenholz, and T. E. Thompson (1976) *Biochemistry* **15**, 4529–4537.
32. E. London and G. W. Feigenson (1981) *Biochemistry* **20**, 1932–1938.
33. E. London and G. W. Feigenson (1981) *Biochim. Biophys. Acta* **649**, 89–97.
34. A. Lopes, J. S. Melo, A. J. Martins, A. L. Maçanita, F. S. Pina, H. Wamhoff, and E. Melo (1995) *Environ. Sci. Tecnol.* **29**, 562–570.
35. L. M. S. Loura, A. Federov, and M. Prieto (2001) *Biophys. J.* **80**, 776–788.
36. S. Mabrey and J. M. Sturtevant (1976) *Proc. Natl. Acad. Sci. USA* **73**, 3862–3866.
37. D. Marsh (1990) *Handbook of Lipid Bilayers*, CRC Press, Boca Raton, FL.
38. L. R. Martin R. B. Avery and R. Welti (1990) *Biochim. Biophys. Acta* **1023**, 383–388.
39. C. R. Mateo, A. A. Souto, F. Amat-Guerri and A. U. Acuña (1996) *Biophys. J.* **71**, 2177–2191.
40. E. C. C. Melo, I. M. G. Lourtie, M. B. Sankaram, T. F. Thompson, and W. L. C. Vaz (1992) *Biophys. J.* **63**, 1506–1512.
41. R. M. R. S. Mesquita, E. Melo, T. E. Thompson and W. L. C. Vaz (2000) *Biophys. J.* **78**, 3019–3025.
42. J. W. Nichols and R. E. Pagano (1981) *Biochemistry* **20**, 2783–2789.
43. J. W. Nichols and R. E. Pagano (1982) *Biochemistry* **21**, 1720–1726.
44. E. Oldfield (1973) *Science* **180**, 982–983 [but see also the response to this comment by S. J. Singer (1973) *Science* **180**, 983].
45. J. A. F. Op den Kamp (1979) *Annu. Rev. Biochem.* **48**, 47–71.
46. R. A. Parente and B. R. Lentz (1985) *Biochemistry* **24**, 6178–6185.
47. A. Pokorny, P. F. F. Almeida, E. C. C. Melo, and W. L. C. Vaz (2000) *Biophys. J.* **78**, 267–280.
48. A. Pralle, P. Keller, E. L. Florin, K. Simons, and J. K. H. Hörber (2000) *J. Cell Biol.* **148**, 997–1007.
49. J. A. Reynolds, C. Tanford, and W. L. Stone (1977) *Proc. Natl. Acad. Sci. USA* **74**, 3796–3799.
50. A. Rietveld and K. Simons (1998) *Biochim. Biophys. Acta* **1376**, 467–479.
51. D. A. Rintoul, M. B. Redd, and B. Wendelburg (1986) *Biochemistry* **25**, 1574–1579.
52. G. J. Schütz, G. Kada, V. P. Pastushenko, and H. Schindler (2000) *EMBO J.* **19**, 892–901.
53. T. B. Shin, R. Leventis, and J. R. Silvius (1991) *Biochemistry* **30**, 7491–7497.
54. J. R. Silvius and F. l'Heureux (1994) *Biochemistry* **33**, 3014–3022.
55. J. R. Silvius, D. del Giudice, and M. Lafleur (1996) *Biochemistry* **35**, 15198–15208.
56. K. Simons and E. Ikonen (1997) *Nature* **387**, 569–572.
57. K. Simons and E. Ikonen (2000) *Science* **290**, 1721–1726.
58. S. J. Singer and G. L. Nicolson (1972) *Science* **175**, 720–731.
59. L. A. Sklar, G. P. Miljanich, and E. A. Dratz (1979) *Biochemistry* **18**, 1707–1716.
60. R. Smith and C. Tanford (1972) *J. Mol. Biol.* **67**, 75–83.
61. C. H. Spink, M. D. Yeager, and G. W. Feigenson (1990) *Biochim. Biophys. Acta* **1023**, 25–33.
62. T. E. Thompson and T. W. Tillack (1985) *Annu. Rev. Biophys. Biophys. Chem.* **14**, 361–386.
63. T. E. Thompson, M. B. Sankaram, R. L. Biltonen, D. Marsh, and W. L. C. Vaz (1995) *Mol. Membr. Biol.* **12**, 157–162.
64. J. F. Tocanne, L. Dupou-Cezanne, A. Lopez, and J. F. Tournier (1989) *FEBS Lett.* **257**, 10–16.
65. W. L. C. Vaz (1992) *Comments Mol. Cell. Biophys.* **8**, 17–36.
66. W. L. C. Vaz (1994) *Biophys. Chem.* **50**, 139–145.
67. W. L. C. Vaz (1995) *Mol. Membr. Biol.* **12**, 39–43.
68. W. L. C. Vaz (1996) in Y. Barenholz and D. Lasic (Eds.), *Handbook of Non-Medical Applications of Liposomes, Vol. 2. Models for Biological Phenomena*, CRC Press, Boca Raton, FL, pp. 51–60.
69. W. L. C. Vaz and P. F. F. Almeida (1993) *Curr. Opin. Struct. Biol.* **3**, 482–488.
70. W. L. C. Vaz, E. C. C. Melo, and T. E. Thompson (1989) *Biophys. J.* **56**, 869–876.
71. W. L. C. Vaz, E. C. C. Melo, and T. E. Thompson (1990) *Biophys. J.* **58**, 273–275.
72. T. Y. Wang and J. R. Silvius (2000) *Biophys. J.* **79**, 1478–1489.
73. T. Y. Wang, R. Leventis, and J. R. Silvius (2000) *Biophys. J.* **79**, 919–933.
74. G. Weber (1952) *Biochem. J.* **51**, 145–155.
75. R. Welti (1982) *Biochemistry* **21**, 5690–5693.
76. R. Welti and D. E. Silbert (1982) *Biochemistry* **21**, 5685–5689.
77. S. H. Wu and H. M. McConnell (1975) *Biochemistry* **14**, 847–854.